SCIENTIFIC REPORTS

OPEN

SUBJECT AREAS:
APPLICATIONS OF AFM
INTRINSICALLY DISORDERED PROTEINS

Received
13 January 2014

Accepted
28 May 2014

Published
20 June 2014

Correspondence and requests for materials should be addressed to L.C. (loredana.casalis@elettra.eu)

* Current address: Fondazione I.R.C.C.S. Istituto Neurologico Carlo Besta, IFOM-IEO-campus, via Adamello, 16, 20139 Milan, Italy.

† Current address: ETH Zürich, Department of Biosystems Science and Engineering, 4058 Basel, Switzerland.

Atomic force microscopy based nanoassay: a new method to study α-Synuclein-dopamine bioaffinity interactions

Stefania Corvaglia[1,2], Barbara Sanavio[1,3]*, Rolando P. Hong Enriquez[3], Barbara Sorce[4]†, Alessandro Bosco[1], Denis Scaini[1,2], Stefania Sabella[4], Pier Paolo Pompa[4], Giacinto Scoles[1,3] & Loredana Casalis[1]

[1]NanoInnovation Laboratory, Elettra Sincrotrone Trieste S.C.p.A., S.S.14 Km 163.5, 34149 Basovizza, Trieste, Italy, [2]Life Science Department, University of Trieste, via Giorgieri 1, I-34127 Trieste, Italy, [3]Department of Biological and Medical Science, University of Udine, Ospedale della Misericordia, Piazzale Santa Maria della Misericordia, 15-33100 Udine, Italy, [4]Center for Bio-Molecular Nanotechnologies@UniLe, Istituto Italiano di Tecnologia, Via Barsanti-73010 Arnesano, Lecce, Italy.

Intrinsically Disordered Proteins (IDPs) are characterized by the lack of well-defined 3-D structure and show high conformational plasticity. For this reason, they are a strong challenge for the traditional characterization of structure, supramolecular assembly and biorecognition phenomena. We show here how the fine tuning of protein orientation on a surface turns useful in the reliable testing of biorecognition interactions of IDPs, in particular α-Synuclein. We exploited atomic force microscopy (AFM) for the selective, nanoscale confinement of α-Synuclein on gold to study the early stages of α-Synuclein aggregation and the effect of small molecules, like dopamine, on the aggregation process. Capitalizing on the high sensitivity of AFM topographic height measurements we determined, for the first time in the literature, the dissociation constant of dopamine-α-Synuclein adducts.

Parkinson's Disease (PD) is one of the most common neurodegenerative diseases that affect the 1–2% of the population after 65 years. Motor disorders that characterize the pathology result from the substantial loss of dopaminergic neurons in the *substantia nigra* and cytoplasmic fibrillaceous inclusions called Lewy bodies (LBs) comprising α-Synuclein (AS) as major constituent are identified in post-mortem PD brains[1]. Due to the preferential vulnerability of dopaminergic neurons in PD, it has been hypothesized a role for dopamine (DA) in the biology of AS[2]. Lansbury et al. suggest that the formation of adducts between DA and AS stabilizes the oligomeric, presumably toxic, protofibrillar form of the protein and inhibits the formation of AS fibrils *in vitro*[3]. The hypothesis that protofibrils are actually the pathogenic species and that fibrils might represent a protective cellular response is in fact consistent with pathological studies that suggest the neuroprotective role of LBs[4,5]. For this reason, DA binding, stabilizing AS protofibrils, could promote PD pathogenesis[6]. Another important function of the DA-modified AS, recently demonstrated, is to block chaperon mediated autophagy[7] although the ensemble of function and effects in living cells is still unclear.

Structurally AS is a small presynaptic protein (14460 Da, 140 residues) that lacks of a specific structure as reported by previous spectroscopic and NMR studies[8–10]. Hence, it is considered an intrinsically disordered protein (IDP), naturally unfolded at physiological conditions. This characteristic is presumably due to the amino acidic composition of the protein that has a high negative charge at neutral pH and low hydrophobicity[11]. The sequence of the protein can be divided into three main regions: residues 1–60 that contain an imperfect repetition of 11 residues with a conserved motif; residues 61–95, the so called NAC region, with high propensity to the aggregation, and residues 96–140, the acidic C-terminal. AS can adopt two stable conformations: alpha-helices when it interacts with cell membranes[12,13] and beta-sheets which characterize amyloid fibrils[14,15]. In both cases, the C-terminal of the protein remains unstructured, probably because of the high negative charge content.

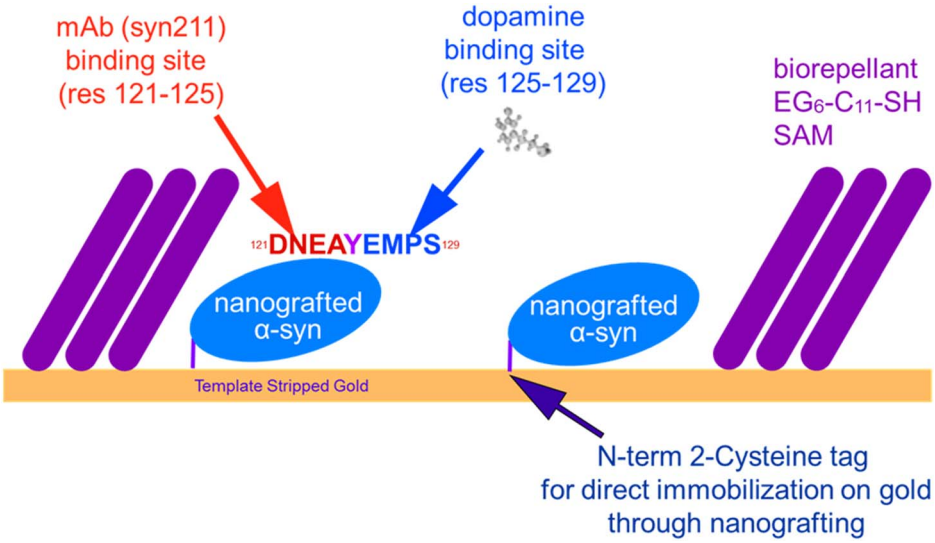

Figure 1 | Schematic representation of the nanografting experiment. A self-assembled monolayer of biorepellent thiols on gold is substituted locally by cysteine-tagged AS. The protein on the surface exposes the C-terminal that contains the specific site for DA binding (^{125}YEMPS^{129}), which overlaps for one amino acid with the site (^{121}DNEAY^{125}) for a AS mAb (syn 211).

Generally, the unfolded characteristics of IDPs and their propensity to aggregate make them difficult to be studied with conventional, solution-based techniques. In particular, the determination of binding affinity parameters is a challenge and, according our knowledge, no data are available in literature. In this context, techniques based on protein immobilization on surfaces can be a valid alternative. Despite the limitation of surface studies, connected to the reduced degree of freedom of the immobilized protein, they can represent a good mean for studying IDPs, and can provide indeed important information about the interaction with small molecules, impossible to measure in bulk. Surface-based assays in which AS is immobilized on a surface, have been used to study AS: Surface Plasmon Resonance (SPR), cyclic voltammetry and standard ELISA measurements of AS aggregation have been reported in literature[16–19]. In all these cases, AS was either immobilized via physisorption or grafted on the surface through a grafted site that is either randomly picked along the sequence and could even be buried in the middle of the protein.

We aimed here at orienting AS on an ultraflat gold surface in a controllable manner, via an engineered di-cysteine tag at the N-terminus. We used Atomic Force Microscopy (AFM) nanolithography, to organize AS to form nanostructures, confined into a self-assembled monolayer of biorepellent alkanethiols ethylene glycol terminated (EG6)[20], on which promoting AS aggregation and studying its interaction with DA. By scanning the AFM tip locally, at high force (about 100 nN) the exchange of molecules of this carpet with the ones of our interest in solution (e.g. di-cysteine modified AS) is favored. The main advantage of this approach, known as *nanografting*[21–24], is that the molecules inside the NAnografted Monolayer (NAM) are all oriented in the same way[25]. The high sensitivity of the AFM topography permits the evaluation of small variations of patch height, with respect to the biorepellent molecular carpet, upon binding of other biomolecules and even small molecules. By exploiting AFM and AFM nanografting using different assay formats, we were then able to create AS nanoassemblies, and to give, for the first time, an estimation of the binding affinity of the DA/AS agglomerates.

Results

1. AS immobilization. To allow for the oriented immobilization of AS, we chose to engineer a specific tag at the N-terminal of the protein. We introduced *via* recombinant techniques two cysteines through which graft the protein on a gold film surface (Fig. 1). In this way, as already demonstrated in our previous works on DNA and protein nanografting[23,25], we expected to obtain a homogeneous distribution of orientation of AS molecules relatively to their grafting site. However, due to the high flexibility and conformational variability of this protein, even a careful orientation of AS on the surface did not provide a mean to fully control a homogeneous distribution of conformations within the patch. Moreover, when the protein was kept in its native state, we did not succeed in nanografting. The reason of this can be twofold: on one side, the unfolded nature of AS in its native state that translates into a low diffusion coefficient; on the other side, the high conformational plasticity of the unfolded AS that could hide the cysteine tag engineered at the N-terminus, making the interaction between the cysteine sulfur group and the gold surface unfeasible. Therefore, we exploited grafting solvents that favor either alpha-helical or beta-sheet conformation. When AS was dissolved in trifluoroethanol to force alpha-helical conformation[26], the grafting was again unsuccessful, probably because of the increased rigidity of the protein in correspondence of a long segment at the N-terminal[27] (similarly to membrane-associated AS conformation) which did not leave the cysteine tag free to react.

Cysteine-tagged AS molecules were successfully immobilized only in solvents that promoted secondary β-sheet structure of AS[26]. We nanografted AS in pure methanol, with an addition of a reducing agent (TCEP) in millimolar concentration, that keeps the di-cysteine tag reduced and the thiols freely available to interact with gold. While in principle disulfides adsorb on gold more efficiently with respect to thiols, in our case protein conformation may play a major role, hindering the disulfide-Au interaction. Even in these conditions, however, the result of AS nanografting was variable. In particular, it was not possible to control *a priori* the grafting density through the variation of fabrication parameters, as we were used to do for example in the case of DNA nanografting. AS nanografted assembly was imaged in contact mode at minimum force (below 100 pN) in buffer solution as a hole of relative height of −1.5 to −0.4 nm with respect to the EG6 thiols SAM, whose measured height was of about 2.6 nm (Fig. S1). These values correspond in fact to a protein height is of 1.1–2.2 nm (with respect to the gold surface), to be compared with the effective AS theoretical value of 1.7–2.1 nm reported in previous works[28]. It is reasonable to think that the molecular densities reached in our AS nanografting experiments were generally low. In addition, we cannot discard a compressing effect induced by the AFM tip during imaging, despite the extremely low load applied.

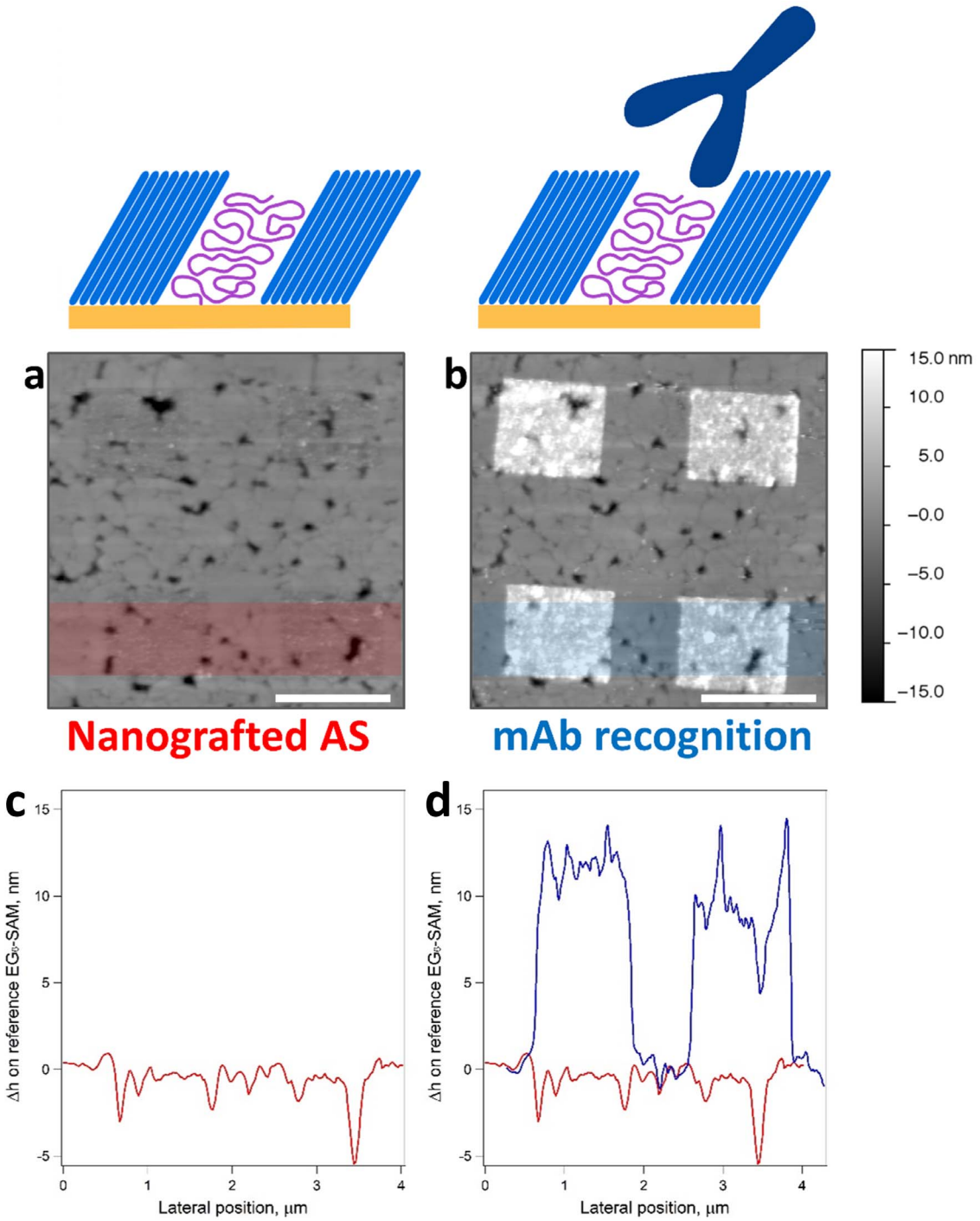

Figure 2 | **AS immobilization.** The AS was nanografted in a reference thiolated SAM (a,c). The presence of the protein was confirmed by the loading of the mAb and a variation in height, compatible with the size of the mAb, was recorded (b), (d). Scale bar 1 μm.

To further prove the success of AS nanografting, we observed that both surface roughness and friction within the nanografted area were different from the surrounding carpet, which is compatible with a modified surface (see Fig. S2). In the experiment shown in Fig. 2, the presence of AS grafted on the surface was confirmed by exposing the surface to a specific mAb (8 nM, clone syn 211) able to recognize an epitope at the C-terminal of the protein (Fig. 2 b,d). We chose a mAb whose recognized epitope spans residues 121–125 (^{121}DNEAY^{125})[29,30] and overlaps for one amino acid the region of residues 125–129 (^{125}YEMPS^{129}), which is known to be a target for DA[19], as shown schematically in Fig. 1. The differential increase in height after mAb binding is compatible with the average dimension of an immunoglobulin G molecule (IgG ca 15–18 nm).

Specificity of the binding was also confirmed with a mock nanografting experiment. An area was "shaved", i.e. the surface was nanografted without the presence of additional thiol, to remove only the preexisting SAM and the bare gold was then incubated with mAb, which did not bind to the selected area (Fig. 3).

2. AS-DA affinity. Having proved that nanografting is an effective way to immobilize AS in confined areas, we tested such micropatterns as sensor to study the binding affinity with DA.

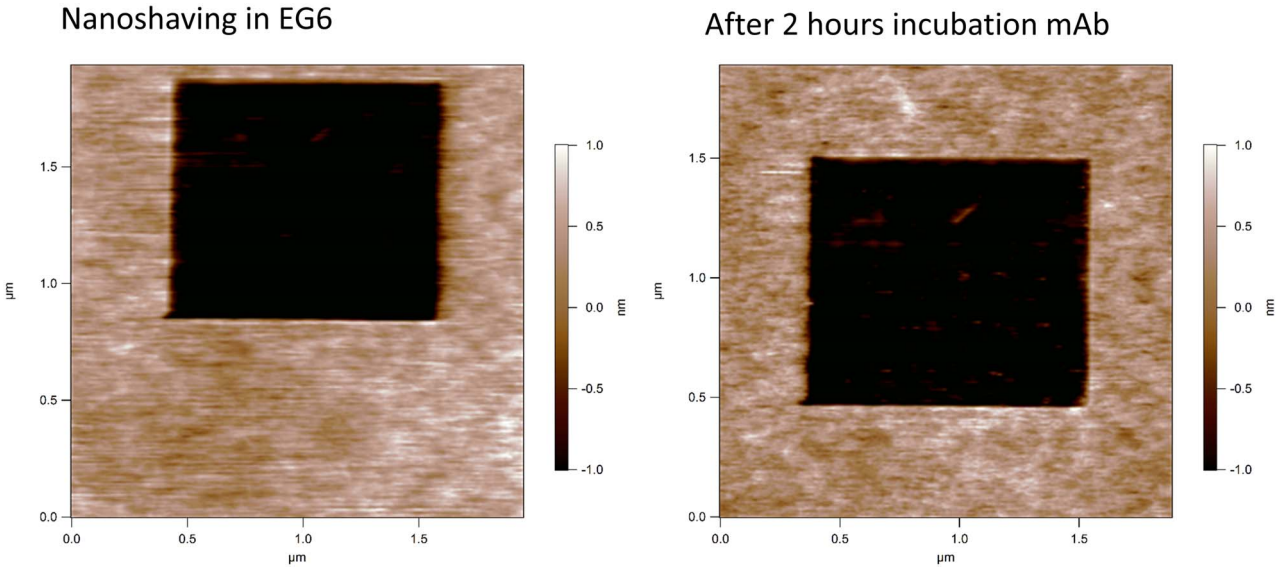

Figure 3 | AFM nanoshaving was performed into an EG6 thiols carpet. A hole was measured by contact mode AFM in liquid (left). The sample was incubated in presence of mAb (clone syn 211) for two hour. AFM imaging suggest no relevant variation in the shaved surface (right), meaning that no aspecific interaction with gold occurred.

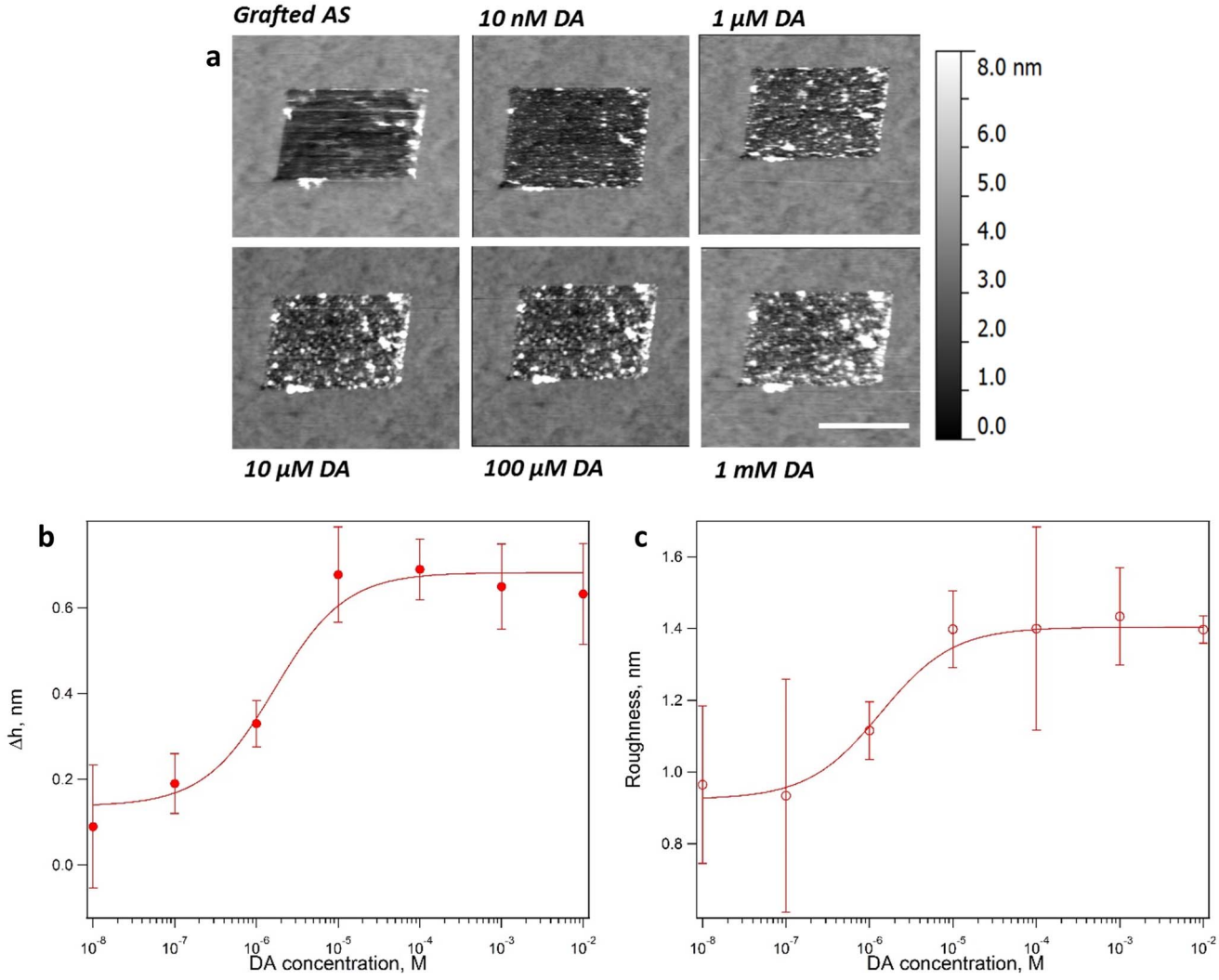

Figure 4 | AS-DA binding experiment. AS change morphologically and some particles appear after increasing DA binding, scale bar 500 nm (a). The loading of DA at increasing concentration lead an evident morphological modification of the protein. This phenomenon was registered by an average increase in the height measured on five different patches. The error is the standard deviation. Fitting with a Langmuir isotherm gave a Kd = 1.7 ± 1.0 μM (b). The same trend is showed by roughness variation analysis. The Kd calculated is 1.4 ± 1.6 μM (c).

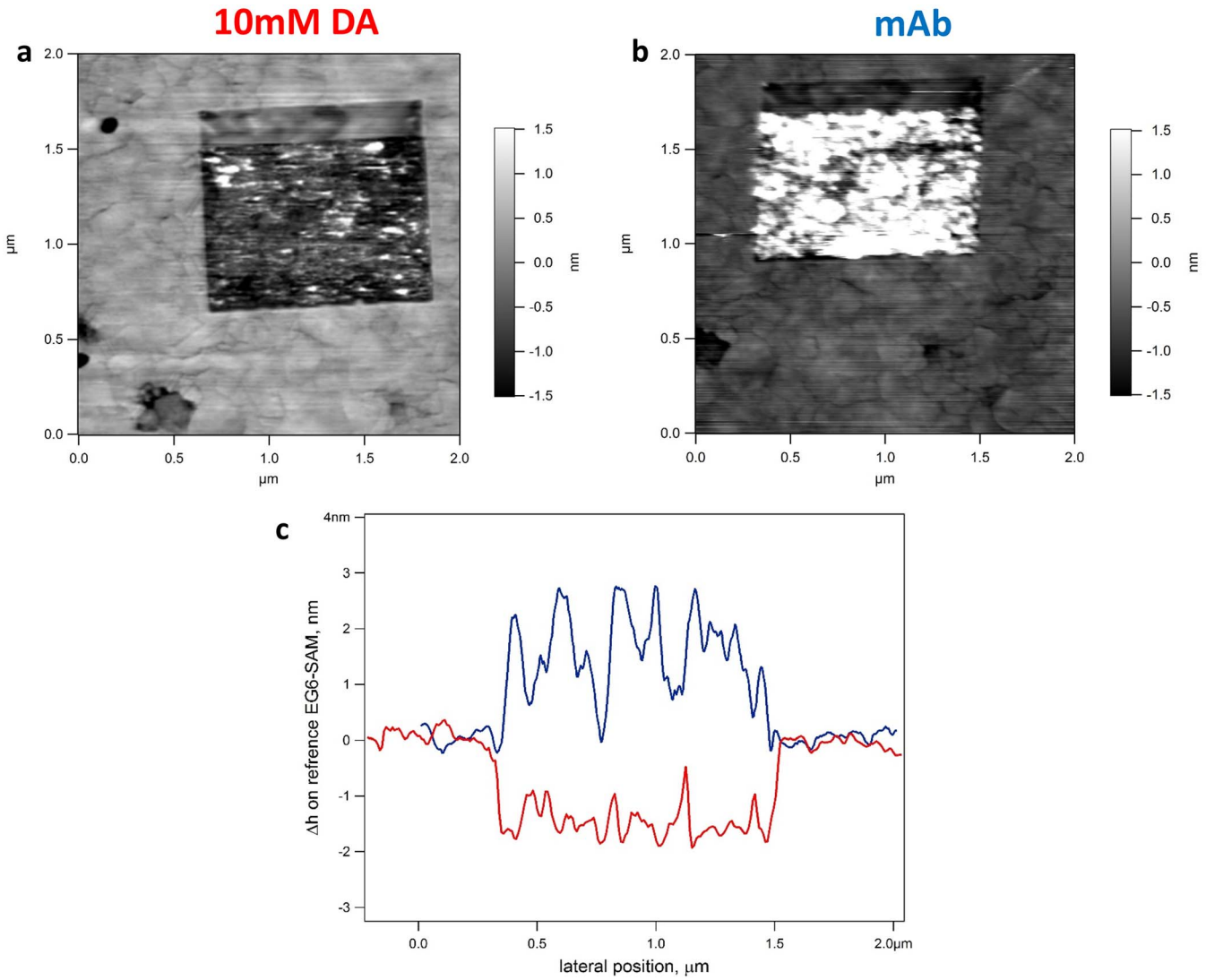

Figure 5 | AS-DA patches recognize the mAb. The AS nanografted patches were treated with 10 mM DA (a). The patches where then incubated with nM concentration of the mAb (b). The topography of the surface increases but it is less than expected (c).

This neurotransmitter is known to interact with residues 120–125 in the C-term tail of the protein, and simultaneously with residues in the NAC region as long-range contact that may stabilize the bound conformation[31,32].

2.1. AS nanostructures to study DA-AS affinity. In order to estimate DA-AS binding affinity, we build a binding assay, measuring the topographical variations of AS nanografted patches incubated with increasing concentration of DA.

An average increase in height, though very moderate, could be recorded, possibly due to an increased rigidity of AS upon DA binding and therefore to an increased resistance to the AFM tip load. More interestingly, the roughness of the nanografted area showed an increase, related to DA binding (Fig. 4). Inspection of the AFM images shows the presence of particles that do not increase in number (they are the same throughout the experiment) upon DA dosing. We analyzed the binding of DA to AS through a sigmoidal dose response of the patch height, obtaining an apparent dissociation constant in the micromolar range (Kd = 1.7 ± 1.0 μM) (Fig. 4b). The same fitting was performed on the roughness variation data, confirming the same trend (Kd = 1.4 ± 1.6 μM) (Fig. 4c). After loading of DA, the sample was treated with nanomolar concentration of mAb syn211 that, as already said, recognizes epitope ^{121}DNEAY^{125}, which overlap for one amino acid (Y125) to the DA binding site. The height of the patches upon mAb loading increases, suggesting that the surface is still covered by the protein with the binding site exposed to the liquid-solid interface, in agreement with previous studies[19]. The measured height (3.3 nm over the AS nanografted patch, Fig. 5) is however lower than expected (Fig. 2 b,d), probably due to the aspecific binding of the mAb.

2.2. mAb-DA displacement assay. AS nanografted patches are recognized by mAb syn211 that binds epitope ^{121}DNEAY^{125}, which overlap for one aminoacid (Y125) to the binding site of DA. This specific mAb was chosen among the many available for its capacity of binding the C-term chain of AS and because of the vicinity of the epitope to the DA binding site. In fact, though the DA binding site overlap for only one amino acid, there is a chance that the conformational change due to the short and long range interaction of DA with ^{125}YEMPS^{129} and residues in the NAC region destabilizes the binding site of the mAb, as is indeed observed experimentally (Fig. 6a). For this reason, we called it as "displacement assay". Since small molecules, like DA, need very precise instrument in order to register their binding, we used the displacement assay to confirm the data obtained in the direct binding assay. In this case, bigger height variations, relatively easy to be measured, can give a more precise estimation of the binding constant. In this assay, the immobilized AS was incu-

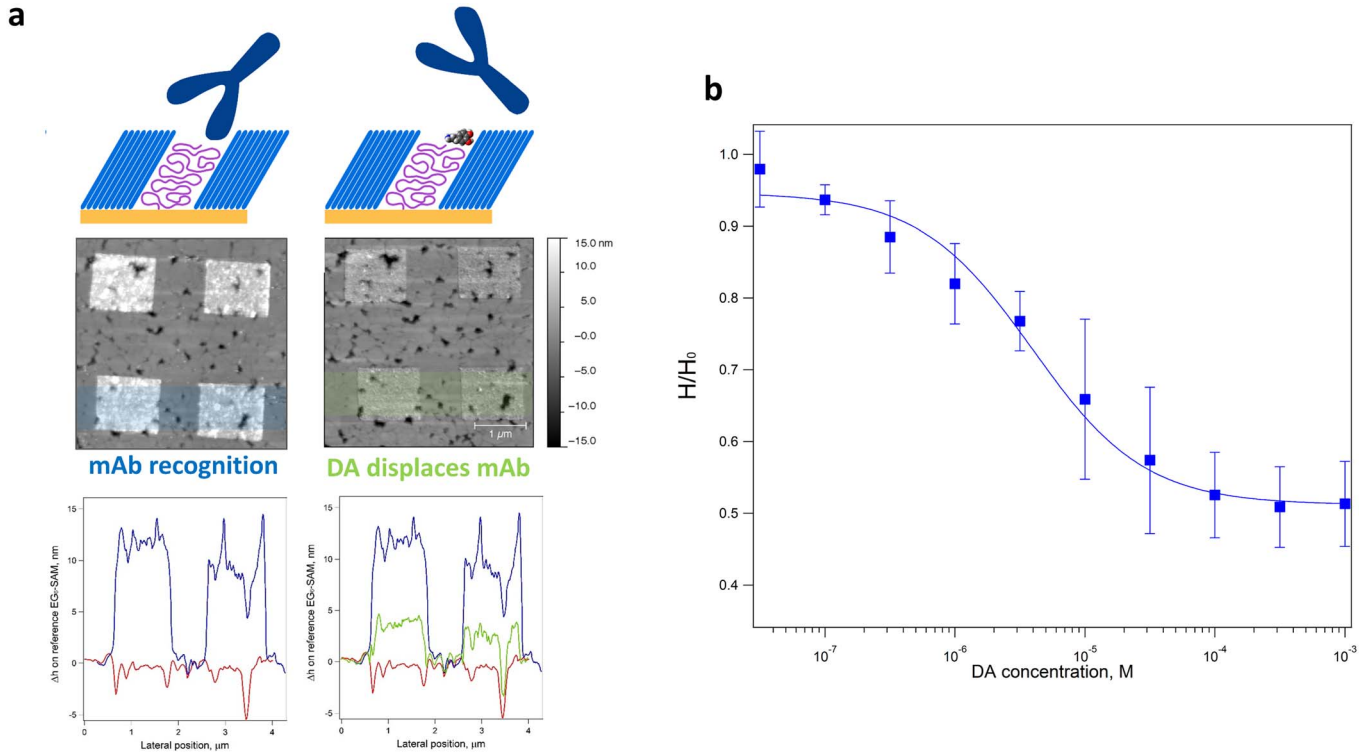

Figure 6 | mAb-DA displacement assay. (a). AS patches recognized by the mAb are incubated with 1 mM DA. The displacement of the mAb is monitored as a decrease in height. (b). The plot reports the average of the absolute heights H of five AS grafted patches during the experiment normalized with respect H_0, the initial height of the patches after mAb incubation, vs DA concentration. Fitting with an inverted Langmuir isotherm gave a Kd = 3.9 ± 1.6 μM. The error is the standard deviation.

bated with DA in the presence of the mAb and the saturated surface was analyzed by AFM topography variations.

After DA addition at increasing concentration, the patches show a decrease in height due to the partial displacement of mAb molecules over the patch (Fig. 6b). A control experiment performed incubating the mAb/AS patches in presence of the bare buffer only (no DA), does not show any height decrease (see Fig. S3). Our speculation is that probably the conformational change occurring upon binding to DA, due to long range interactions, can destabilize the AS/mAb binding. This hypothesis is supported by theoretical modeling (see supporting informations) that suggests a weak interaction of AS with the YEMPS site, and therefore a key role of long range interactions in the stabilization of DA binding.

Plotting the measured absolute height (normalized over the height of mAb saturated AS patches) *vs* DA concentration, we obtain an inverted Langmuir isotherm from which it is possible to calculate the Kd value as the concentration of DA that causes half-maximal displacement of the mAb. The value obtained of 3.9 ± 1.6 μM is in good agreement with the experimental Kd calculated in the direct assay previously described. As observed by the data plot, at saturation the mAb is not completely displaced from the surface. This phenomenon suggests that some mAb are interacting with AS through nonspecific binding sites, as suggested also by the previous experiment (Fig. 5b).

3. AS nanostructures to promote the supramolecular assembly formation and to study the effect of DA on them. Finally, results about the potential use of this assay to study the early stages of the AS aggregation are presented. In this case, AS nanografted patches (Fig. 7a) were incubated with a solution containing recombinant AS to promote AS aggregation. We observed a time-dependent topographic height increase over the AS patches versus incubation time (24–48–72 hours, Fig. 7 b, c, d) suggesting a local interaction between AS molecules. The addition of highly concentrated DA (20 μM, close to the saturation point) disrupts these aggregates after 30 minutes incubation, probably stabilizing small oligomers, observable as round spheres by AFM imaging (Fig. 7e). Further addition of AS molecules plus DA after DA treatment does not show any increase in patch height after 24 hours incubation, confirming the stable binding of DA on the protein (Fig. 7f). The analysis of the roughness of the patches confirms the formation of aggregates on the surface (Fig. 7h). These data support the hypothesis that DA and its oxidation products, such as dopaminochrome, interacting with the ^{125}YEMPS^{129} region, inhibit the formation of AS aggregates. This could suggest that DA binding causes a conformational rearrangement in the AS molecules, due to the interaction with distal residues at the N-terminal, leading to an off-pathway intermediate, unable to produce aggregates.

Discussion

AS is part of a family of proteins called IDPs. They are characterized by a total or partial lack of a three dimensional conformation and are prone to aggregation. These unfolded characteristics make difficult the study of these proteins with conventional techniques. In this work, we demonstrated that nanografting is a useful tool to immobilize AS and study the interactions that affect these proteins. The orientation of the molecules on a confined surface and the high precision in the AFM measurements, permitted the calculation of the affinity between AS and small molecules like DA speculating a conformational rearrangement of the protein during this process. We were also able to calculate for the first time the dissociation constant between AS and DA that is in the micromolar range. Once we demonstrated a competition between DA and the mAb (clone syn 211) to bind to AS, probably due to the close proximity and the partial overlapping of the two binding sites, our assay was exploited also for displacement studies. The observed partial displacement of the mAb from its AS binding site upon DA incubation was attributed to a rearrangement of the three dimensional structure

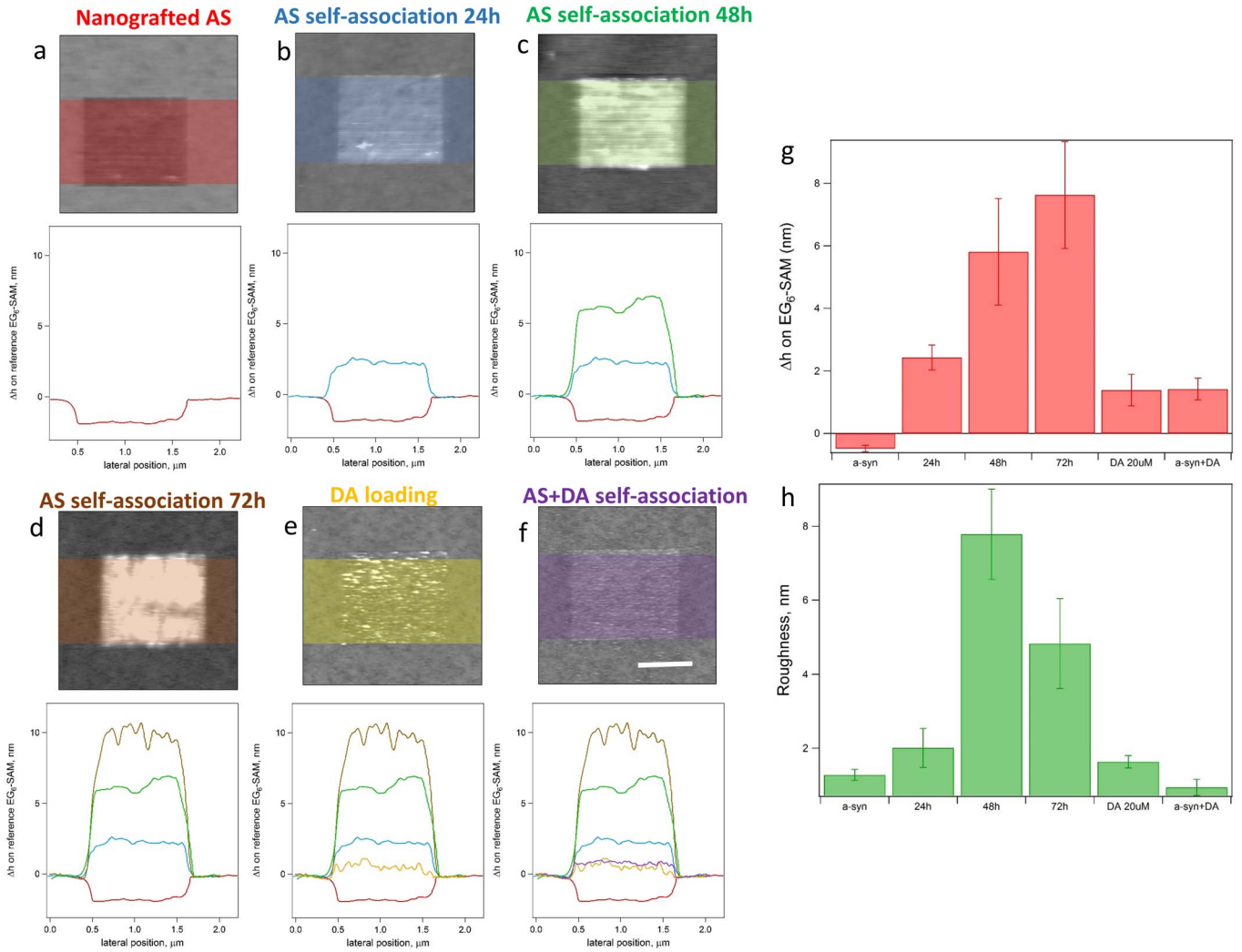

Figure 7 | AS patches were incubated in presence of AS. The surface was monitored over time by topographic AFM measurement (a), (b), (c), (d). Finally, the effect of DA was evaluated. DA interacts with the AS self-association site disrupting the aggregates formed in 72 hours, stabilizing small oligomers (e). Such binding is stable and prevents the self-association in presence of AS molecules also after 24 hours of incubation (f). The aggregation process and the disaggregation are reflected by the topography (g) and the roughness (h) of the surface. The values are calculated as the average of five different patches, the error is the standard deviation. Scale bar 500 nm.

of the protein due to effective interaction of DA on the expected binding site ^{125}YEMPS^{129} and to long-range interactions. Our displacement assay gave us the possibility to measure the AS-DA binding affinity from large topographic height variation signals, relatively easy to be measured by AFM. This assay confirmed the micromolar dissociation constant calculated in the direct assay, supporting the validity and the precision of our technique for binding studies of small molecules. With the help of the theoretical modeling, we explored the role of the ^{125}YEMPS^{129} site of AS in the binding with DA. We observed that the theoretical dissociation constant is higher than the experimental one (from mM to μM). These results strengthen the hypothesis that non-covalent contacts with residues of the NAC region, stabilizing the AS/DA adduct increase the affinity of the binding.

Finally, we demonstrated that our assay could represent a valid alternative for the study of the early stages of the aggregation process. In particular, our approach was used to confirm the effect of dopamine on these structures, able to dissolve self-associated AS.

In conclusion, we demonstrated that the combination of AFM nanografting and topographic readout is a valid tool for the determination of the affinity binding of unstructured proteins, such as AS, with small molecules and for testing the effect of small molecules on the early stages of the aggregation process.

Methods

Materials and instrumentation. EG6-thiols, HS-$(CH_2)_{11}$-$(OCH2CH2)_6$-OH, were purchased from Prochimia Surfaces (Poland). KCl, TRIS (2-Amino-2-hydroxymethyl-propane-1,3-diol), TCEP (*tris*(2-carboxyethyl)phosphine), sodium acetate, methanol and ethanol (99.8% purity) were all provided by Fluka and Sigma Aldrich, (Milan, Italy). All the solutions were prepared in ultrapure 18.2 MΩ·cm water (Milli-Q, Millipore SpA, Milan, Italy), and filtered with a sterile syringe-filter (0.22 μm) prior to use. All other reagents were of analytical grade. All AFM experiments were carried out with conventional AFMs using a XE-100 (Park System, former PSIA, Korea) and a MFP3D Stand Alone AFM, (Asylum Research, Santa Barbara, CA) working in contact mode. For nanografting commercially available silicon cantilevers (NSC19, Mikro- Masch, Poland, nominal spring constant 0.6 nN/nm, tip radius <10 nm) were chosen. For CM-AFM imaging purposes, a soft cantilever (CSC38B, MikroMasch, Poland, nominal spring constant, 0.03 nN/nm, tip radius <10 nm) was used.

Substrate and monolayer preparation. An ultra-flat gold surface was prepared following the *Template Stripped Gold* (TSG) procedure described by Wagner *et al*[33]. Briefly, a layer of gold was evaporated on freshly cleaved mica sheets (clear ruby muscovite, Goodfellow Cambridge Limited, Huntingdon, England) or on a Si(100) wafer using an electron beam gold evaporator. Gold films were deposited at a rate of ~0.1 nm/s and a chamber pressure of about 10^{-6} mbar until a thickness of 100 nm

was reached. These films were fixed to Si(100) wafer pieces with a drop of SU8-100 (MicroChem Corp., MA), and the polymer was then cured (baked 5 h at 95°C, exposed 20 min under a 70 μW/cm^2, 462 nm UV lamp, and baked at least 3 hours at 95°C). They were then separated at the gold–mica (or gold-Si) interface by peeling immediately before functionalization. This procedure made gold substrates with a flat surface morphology, reproducing the atomically flat mica surface. Samples are then soaked in a freshly prepared 300 μM solution of EG6-terminated thiols in ethanol. The substrates were incubated overnight in the dark at room temperature. In this way, a self-assembled monolayer (SAM) of thiolated molecules covers the ultra-flat gold surface. AFM test measurements confirmed a roughness of the substrate in the range of 0.3–0.4 nm.

Recombinant Di-Cysteine AS expression and purification. In order to remove most tags at the end of the purification process, we used Profinity eXact™″ fusion-tag system (Bio-Rad Laboratories, Hercules, Calif.) which uses an immobilized subtilisin protease to carry out affinity binding and tag cleavage to produce Di-Cysteine AS. The human AS cDNA was isolated by pUC57-α-syn vector purchased by GenScript. The following primers were used: 5′ CGAAAGCTTTGACTTCT TGCTGCGATGTATTC ATGAAAGG 3′ containing nucleotides coding for Thr-Ser linker to obtain an optimal cleavage during the purification step, nucleotides coding for two Cys and restriction site for *Hind III* and 3′ TACCCATGGTTAGGCT-TCAGGTTCGTAGTCTT 5′ containing the restriction site for *NcoI*. The α-Syn cDNA was cloned into the *Hind III* and *NcoI* restriction sites of the bacterial expression vector pPAL7. BL21(DE3) *E. coli* were transfected with pPAL7/Cys-α-syn plasmid, and expression was induced by the addition of isopropyl β-D-thiogalactopyranoside (IPTG). Cells were harvested, resuspended in 10 mM Tris, pH 8, 1 mM EDTA, 1 mM PMSF (1/10 culture volume), and lysed by freezing in liquid nitrogen followed by thawing and probe sonication. The di-Cyst AS protein was purified by size-exclusion chromatography (Superdex 200 10/300 GL, Amersham Bioscences) with 50 mM sodium phosphate buffer pH 7.4, 300 mM NaCl. After the collected fraction was purified by using Profinity exact resin (Bio-Rad Laboratories, Hercules, Calif.). The protein purified was verified by SDS PAGE 2–15% and then lyophilized. Di-Cyst AS protein was determinated to be ca. 97% pure by SDS-PAGE.

AFM Nanografting and imaging. Nanografting experiments were performed as follows: a freshly SAM passivated gold substrate was rinsed with ethanol and fixed in an AFM closed liquid cell. The gold surface was scratched with a worn out AFM tip to have a recognition point onto the surface to facilitate finding back the nanostructures. The liquid cell was filled with the nanografting solution that contains 3 mM cysteine-tagged AS in methanol with the addition of 1 mM TCEP dissolved in methanol. The patches were obtained scanning the desired area at high load (about 100 nN) and at a scan rate about 2 Hz. In this way local excange between the EG6-thiolated molecules and the protein in solution is promoted. During nanografting procedure, patches of about 1 μm^2 (512 × 512 pixels) were fabricated. The liquid cell was abundantly washed with 10 mM TRIS, 150 mM KCl, pH 7.4 after the incubation time of every step of the experiments. The imaging was performed in contact mode in the same buffer at minimum load forces (below 100 pN).

Dopamine (DA) binding. Dopamine (Sigma Aldrich) was freshly dissolved and incubated with increasing concentration (from 10 nM to 10 mM) in buffer 20 mM sodium acetate, 150 mM KCl pH 5.5, to minimize auto-oxidation. The differential height was used as the response signal and fitted to a Langmuir isotherm[35], that describes the binding of a ligand to a macromolecule, in Igor Pro (Wavemetrics, Inc.). The topographic measurements were performed after 30 minutes incubation, time sufficient for the diffusion and the binding of the DA. A mAb (8 nM, syn clone 211, Sigma Aldrich)[29] was used to recognize AS patches. The antibody was diluted in buffer 10 mM TRIS, 150 mM KCl, pH 7.4 and incubated for 2 hours.

Displacement assay. Nanografted AS patches were incubated in presence of a solution of the mAb (syn clone 211, Sigma Aldrich)[29] 8 nM, dissolved in 10 mM TRIS, 150 mM KCl, pH 7.4 and incubated for two hours. The topographic measurements were performed after 30 minutes incubation, time sufficient for the diffusion and the binding of the DA. The differential height was used as the response signal and fitted to an inverted Langmuir isotherm[35], that describes the non-competitive binding of a second ligand to a macromolecule, in Igor Pro (Wavemetrics, Inc.).

AS self-association. Recombinant human AS histine-tagged (Sigma Aldrich) was freshly dissolved at 3.5 μM concentration in buffer 10 mM TRIS, 150 mM KCl, pH 7.4. As reported in literature the presence of the histidine does not affect significantly the AS aggregation[34]. AS nanografted patches were incubated in presence of the histidine tagged AS at different times (24, 48, 72 hours). 20 μM DA was added and incubated for 30 minutes over the self-associated AS patches. The further addition of 3.5 μM AS in presence of DA for 24 hours did not increase the height of the patches.

Images analysis. For each experiment were fabricated multiple patches that contribute to the experiment statistic. For every patch the average height was calculated from the average profile and together with the standard deviation. Topographic images of the patches are then analyzed in term of pixel distribution (region analysis) in order to get the height value related to the patch at each single step of the experiments. The AFM instrument proprietary software (XEI, Park System, and MFP3D, Asylum Research) as well as free open source software, Gwyddion (www.gwyddion.net), were used.

1. Goedert, M. Alpha-synuclein and neurodegenerative diseases. *Nat. Rev. Neurosci.* **2**, 492–501 (2001).
2. Galvin, J. E. Interaction of alpha-synuclein and dopamine metabolites in the pathogenesis of Parkinson's disease: a case for the selective vulnerability of the substantia nigra. *Acta Neuropathol.* **112**, 115–26 (2006).
3. Conway, K. a., Rochet, J. C., Bieganski, R. M. & Lansbury, P. T. Kinetic stabilization of the alpha-synuclein protofibril by a dopamine-alpha-synuclein adduct. *Science* **294**, 1346–9 (2001).
4. Tompkins, M. M., Basgall, E. J., Zamrini, E. & Hill, W. D. Apoptotic-like changes in Lewy-body-associated disorders and normal aging in substantia nigral neurons. *Am. J. Pathol.* **150**, 119–31 (1997).
5. Goldberg, M. S. & Lansbury Jr, P. T. Is there a cause-and-effect relationship between alpha-synuclein fibrillization and Parkinson's disease? *Nat. Cell Biol.* **2**, E115–E119 (2000).
6. Conway, K. A., Harper, J. D. & Lansbury, P. T. Fibrils Formed in Vitro from alpha-Synuclein and Two Mutant Forms Linked to Parkinson's Disease are Typical Amyloid. *Biochemistry* **39**, 2552–2563 (2000).
7. Martinez-Vicente, M. *et al.* Dopamine-modified α-synuclein blocks chaperone-mediated autophagy. *J. Clin. Invest.* **118**, 777–788 (2008).
8. Rivers, R. C. *et al.* Molecular determinants of the aggregation behavior of alpha - and beta -synuclein. *Protein Sci.* **17**, 887–898 (2008).
9. Bertoncini, C. W. *et al.* Release of long-range tertiary interactions potentiates aggregation of natively unstructured alpha-synuclein. *Proc. Natl. Acad. Sci. U. S. A.* **102**, 1430–1435 (2005).
10. Dedmon, M. M., Lindorff-Larsen, K., Christodoulou, J., Vendruscolo, M. & Dobson, C. M. Mapping long-range interactions in alpha-synuclein using spin-label NMR and ensemble molecular dynamics simulations. *J. Am. Chem. Soc.* **127**, 476–7 (2005).
11. Uversky, V. N., Gillespie, J. R. & Fink, a L. Why are "natively unfolded" proteins unstructured under physiologic conditions? *Proteins* **41**, 415–27 (2000).
12. Davidson, W. S., Jonas, a., Clayton, D. F. & George, J. M. Stabilization of alpha-synuclein secondary structure upon binding to synthetic membranes. *J. Biol. Chem.* **273**, 9443–9 (1998).
13. Dikiy, I. & Eliezer, D. Folding and misfolding of alpha-synuclein on membranes. *Biochim. Biophys. Acta* **1818**, 1013–8 (2012).
14. Vilar, M. *et al.* The fold of a-synuclein fibrils. *Proc. Natl. Acad. Sci.* **105**, 8637–8642 (2008).
15. Apetri, M. M., Maiti, N. C., Zagorski, M. G., Carey, P. R. & Anderson, V. E. Secondary structure of alpha-synuclein oligomers: characterization by raman and atomic force microscopy. *J. Mol. Biol.* **355**, 63–71 (2006).
16. Kang, T. *et al.* Characterization of surface-confined alpha-synuclein by surface plasmon resonance measurements. *Langmuir* **22**, 13–7 (2006).
17. Van Geel, W. J. A. *et al.* A more efficient enzyme-linked immunosorbent assay for measurement of alpha-synuclein in cerebrospinal fluid. *J. Neurosci. Methods* **168**, 182–185 (2008).
18. An, Y. *et al.* A photoelectrochemical immunosensor based on au-doped TiO2 nanotube arrays for the detection of α-synuclein. *Chem. - A Eur. J.* **16**, 14439–14446 (2010).
19. Norris, E. H. *et al.* Reversible inhibition of alpha-synuclein fibrillization by dopaminochrome-mediated conformational alterations. *J. Biol. Chem.* **280**, 21212–9 (2005).
20. Ostuni, E., Chapman, R. G., Holmlin, R. E., Takayama, S. & Whitesides, G. M. A survey of structure - property relationships of surfaces that resist the adsorption of protein. *Langmuir* **17**, 5605–5620 (2001).
21. Liu, M., Amro, N. A. & Liu, G. Nanografting for surface physical chemistry. *Annu. Rev. Phys. Chem.* **59**, 367–386 (2008).
22. Staii, C., Wood, D. & Scoles, G. Ligand-induced structural changes in maltose binding proteins measured by atomic force microscopy. *Nano Lett.* **8**, 2503–2509 (2008).
23. Bano, F. *et al.* Toward multiprotein nanoarrays using nanografting and DNA directed immobilization of proteins. *Nano Lett.* **9**, 2614–18 (2009).
24. Sanavio, B. *et al.* Oriented immobilization of prion protein demonstrated via precise interfacial nanostructure measurements. *ACS Nano* **4**, 6607–16 (2010).
25. Mirmomtaz, E. *et al.* Quantitative Study of the Effect of Coverage on the Hybridization Efficiency of Surface-Bound DNA Nanostructures. *Nano* **8**, 4134–4139 (2008).
26. Munishkina, L. A., Phelan, C., Uversky, V. N. & Fink, A. L. Conformational behavior and aggregation of α-synuclein in organic solvents: Modeling the effects of membranes. *Biochemistry* **42**, 2720–2730 (2003).
27. Anderson, V. L., Ramlall, T. F., Rospigliosi, C. C., Webb, W. W. & Eliezer, D. Identification of a helical intermediate in trifluoroethanol-induced alpha-synuclein aggregation. *PNAS* **107**, 18850–18855 (2010).
28. Nath, S., Meuvis, J., Hendrix, J., Carl, S. a. & Engelborghs, Y. Early aggregation steps in alpha-synuclein as measured by FCS and FRET: evidence for a contagious conformational change. *Biophys. J.* **98**, 1302–11 (2010).
29. Giasson, B. I. *et al.* A panel of epitope-specific antibodies detects protein domains distributed throughout human alpha-synuclein in Lewy bodies of Parkinson's disease. *J. Neurosci. Res.* **59**, 528–533 (2000).

30. Croisier, E. *et al.* Comparative study of commercially available anti-alpha-synuclein antibodies. *Neuropathol. Appl. Neurobiol.* **32**, 351–356 (2006).
31. Herrera, F. E. *et al.* Inhibition of alpha-synuclein fibrillization by dopamine is mediated by interactions with five C-terminal residues and with E83 in the NAC region. *PLoS One* **3**, e3394 (2008).
32. Dibenedetto, D., Rossetti, G., Caliandro, R. & Carloni, P. A molecular dynamics simulation-based interpretation of nuclear magnetic resonance multidimensional heteronuclear spectra of α-synuclein·dopamine adducts. *Biochemistry* **52**, 6672–83 (2013).
33. Hegner, M., Wagner, P. & Semenza, G. Ultralarge atomically flat template-stripped Au surfaces for scanning probe microscopy. *Surf. Sci.* **291**, 39–46 (1993).
34. Meuvis, J., Gerard, M., Desender, L., Baekelandt, V. & Engelborghs, Y. The conformation and the aggregation kinetics of a-Synuclein depend on the proline residues in Its C-terminal region. *Biochemistry* **49**, 9345–9352 (2010).
35. Copeland, R. A. *Enzymes.* (Wiley-VCH, Inc., 2000).

Acknowledgments

The authors gratefully thank Luca Ianeselli, Elena Ambrosetti and Pietro Parisse for useful discussions. This work was supported by the ERC grant "Monalisa Quidproquo" to G.S. and L.C. and FIRB 2008 "NanoMosquito" to D.S.

Author contributions

S.C. performed all the experiments, analyzed data and wrote the manuscript draft. B.S. performed some preliminary experiments, contributed with helpful suggestions and revised the manuscript. R.H. performed the simulations. B.S., S.S. and P.P. prepared and purified the cysteine tagged α-Synuclein. A.B. and D.S. contributed to the experiments with constructive advices and manuscript revisions. G.S. and L.C. supervised the project and revised the manuscript. All authors read and approved the manuscript.

Additional information

Supplementary information accompanies this paper at http://www.nature.com/scientificreports

Competing financial interests: The authors declare no competing financial interests.

How to cite this article: Corvaglia, S. *et al.* Atomic force microscopy based nanoassay: a new method to study α-Synuclein-dopamine bioaffinity interactions. *Sci. Rep.* **4**, 5366; DOI:10.1038/srep05366 (2014).